then be attributed to a compound-nucleus-evaporation mechanism, while the long "tail" at higher energies must be due to a different mechanism—perhaps a direct interaction of the helium ion with one or two neutrons.

Such a non-conpound-nucleus mechanism implies the transfer of less momentum to the reaction product, and hence implies that the recoil collection efficiency might be less than expected. However, the Bk^{249} target deposit was sufficiently thin that recoils with much less than the full momentum would escape. (This was shown by measuring in several bombardments the small amount of Bk^{249} ejected from the target by elastic and inelastic scattering processes, which gives a very sensitive measure of the thickness of the target.[14]) In addition, the measurement of the yield of Cf^{246} from the Cm^{244} added to the target automatically compensated for any such effects insofar as they occurred equally for nuclear reactions of Bk^{249} and for the $(\alpha,2n)$ reaction of Cm^{244}.

[14] A. Chetham-Strode (unpublished).

ACKNOWLEDGMENTS

It is a pleasure to thank the crew of the 60-inch cyclotron for their extremely careful and skillful operation of the machine during some 200 hours of bombardments. We wish to thank Lennart Holm for participation in the later stages of this work, and Professor Glenn T. Seaborg for his continued interest.

We are especially indebted to Thomas C. Parsons for the production and primary purification of the Bk^{249} target sample.

PHYSICAL REVIEW VOLUME 104, NUMBER 5 DECEMBER 1, 1956

Interaction of 1.0-, 1.77-, 2.5-, 3.25-, and 7.0-Mev Neutrons with Nuclei*

J. R. Beyster, M. Walt,† and E. W. Salmi
Los Alamos Scientific Laboratory, Los Alamos, New Mexico

(Received August 1, 1956)

The differential cross sections for elastic scattering of 2.5-Mev neutrons by Al, Fe, Zr, Sn, Ta, and Bi were measured over the angular range from 15° to 160°. At 7.0 Mev similar measurements were made for Be, C, Al, Fe, Zr, Sn, Ta, and Bi at angles ranging from 12° to 150°. Inelastic collision cross sections were determined by sphere transmission measurements for a number of elements at 1.0-, 1.77-, 2.5-, 3.25-, and 7-Mev neutron energies.

By using an optical model of the nucleus, cross sections for elastic scattering and for compound nucleus formation were calculated. With suitable choices of the optical model parameters the calculated cross sections are in reasonable agreement with the experimental values.

I. INTRODUCTION

PREVIOUS measurements of fast-neutron interactions with nuclei have been interpreted with considerable success in terms of an optical model of the nucleus.[1–4] This model, which represents the nucleus by a complex potential well, can be used to calculate the total cross section, the differential cross section for elastic scattering, and the cross section for compound nucleus formation. Most calculations of this type have been done using a square potential well. Although the qualitative features of the cross-section variations with energy and with atomic weight were reproduced, this model failed in one notable respect. Namely, the cross sections for compound nucleus formation were significantly smaller than the experimental data indicated.[2] The source of trouble was thought to be the sharp edge of the potential well, and rounding of the potential well was proposed. This refinement is identical to that introduced by Woods and Saxon[5] to interpret proton scattering experiments. The cross-section information available some time ago was extensive enough to indicate the limitations of the complex, square-well model. However, it has been apparent that additional cross-section data would be helpful in testing the more refined models of the nucleus since very often the available information has not been sufficient to define a unique set of nuclear parameters.

The investigation reported here was undertaken to measure differential cross sections for elastic scattering and inelastic collision cross sections in energy regions where experimental data were not available. Several measurements have been made in the past on the angular distributions of elastically scattered neutrons.[2,6–9] However, very limited experimental data

* Work performed under the auspices of the U. S. Atomic Energy Commission.

† Now at Lockheed Aircraft Corporation, Palo Alto, California.

[1] Feshbach, Porter, and Weisskopf, Phys. Rev. 96, 448 (1954).

[2] M. Walt and J. R. Beyster, Phys. Rev. 98, 677 (1955).

[3] Bjorklund, Fernbach, and Sherman, Phys. Rev. 101, 1832 (1956).

[4] J. O. Elliot, Phys. Rev. 101, 684 (1956).

[5] R. D. Woods and D. S. Saxon, Phys. Rev. 95, 577 (1954); 101, 506 (1956).

[6] W. D. Whitehead and S. C. Snowden, Phys. Rev. 92, 114 (1953); 94, 1267 (1954). Willard, Bair, and Kington, Phys. Rev. 98, 669 (1955); A. Langsdorf and R. O. Lane, Phys. Rev. 99, 621 (1955); W. J. Rhein, Phys. Rev. 98, 1300 (1955); I. L. Morgan,

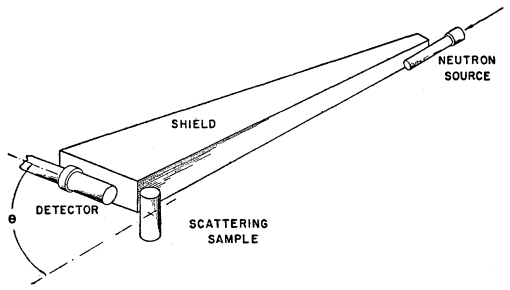

FIG. 1. The experimental arrangement for differential cross-section measurements.

exist in the neutron energy range between 1.5 and 3.7 Mev and between 4.1 and 14.0 Mev. The measurements at 2.5 and 7 Mev reported here were undertaken to obtain information in these regions. Similarly, few measurements of inelastic collision cross sections exist for energies between 1 and 4 Mev and between 4.5 and 14 Mev. The energy region between 1 and 4 Mev is of interest since for most elements the inelastic cross section rises rapidly with increasing energy in this region. Between 4.5 and 14 Mev recent measurements[10] have given values which for some elements are not in good agreement with those obtained in earlier integral experiments.[11] To remove this uncertainty and to establish the energy dependance of the inelastic collision cross section, measurements were made on many elements at 1.0-, 1.77-, 2.5-, 3.25-, and 7.0-Mev neutron energies.

The comparison of the optical-model predictions with experiment is somewhat ambiguous at neutron energies below several Mev. As the neutron energy increases, this ambiguity becomes less important so that the measurements at 7.0-Mev neutron energy were especially desirable for the comparison of theory and experiment.

In Sec. II of this paper the experimental procedure used in obtaining differential cross sections for elastic scattering and inelastic collision cross sections is briefly discussed. The results of the measurements are presented in Sec. III. In Sec. IV the experimental values are compared with cross sections calculated using a complex, diffuse-edge nuclear potential, and values of the well parameters are discussed.

II. EXPERIMENTAL PROCEDURE

A. Measurement of Angular Distributions

Previous measurements[2,6,7] at 1-Mev and near 4-Mev neutron energy indicated that the angular distributions of neutrons scattered by elements with almost the same atomic weight were nearly identical. Therefore, in the present experiment a limited number of elements were chosen at intervals in the periodic table to determine the variation of differential cross section with atomic weight. At 2.5 Mev the elements studied were Al, Fe, Zr, Sn, Ta, and Bi while at 7.0 Mev the differential cross sections of Be, C, Al, Fe, Zr, Sn, Ta, and Bi were obtained. The general method used in measuring the angular distributions of elastically scattered neutrons has been described in previous publications.[2,7] Briefly, the method consists of placing a cylindrical scattering sample in a flux of monoenergetic neutrons and observing with an energy-sensitive detector the intensity of the scattered flux at various angles. From the ratio of the counting rates of the detector in the direct flux and in the scattered neutron flux and from a knowledge of the scatterer mass and of the geometry, the differential cross section can be obtained.

Figure 1 indicates the experimental geometry. The distance between neutron source and scatterer was about 40 cm. The scattering samples were cylinders 6 cm in length with diameters varying from about 1.5 cm to 2.5 cm. The diameters were chosen so that only about 15% of the neutrons which interacted with the scatterer had more than one collision before leaving the sample. To measure the scattering at angles of 30° or greater, the detector was placed about 12 cm from the axis of the scattering sample. Observations at angles less than 30° were made with the sample to detector distance increased to about 25 cm. Shielding material was placed between the neutron source and the detector to reduce the counting rate produced by neutrons coming directly from the source. The background was measured by observing the counting rate with the scattering sample removed.

Corrections were made to the measured data for differences in the efficiency with which direct and scattered neutrons were detected. This correction was made by calculating the loss in energy at each scattering angle for each element and comparing the detector sensitivity at this final energy with the detector sensitivity for neutrons of the primary energy. Corrections were also made for the attenuation of the primary flux in the scattering sample, for multiple scattering, and for the finite angular resolution of the geometry. The analytical correction procedure usually employed to remove the multiple scattering effects could not easily be applied to the scattering data at 7 Mev for elements heavier than aluminum because of the complicated shapes of the angular distributions. Therefore, the multiple scattering corrections for Fe, Zr, Sn, Ta, and Bi at 7 Mev were made by Monte Carlo calculations performed on the Los Alamos MANIAC digital computer. The corrections for finite angular resolution were made by an approximate unfolding of the counter resolution function from the experimental angular distributions.

Phys. Rev. **99**, 621 (1955); Allen, Walton, Perkins, Olson, and Taschek, Phys. Rev. **104**, 731 (1956).

[7] M. Walt and H. H. Barschall, Phys. Rev. **93**, 1062 (1954).

[8] J. H. Coon and R. W. Davis, Phys. Rev. **94**, 785 (1954).

[9] W. G. Cross and R. G. Jarvis, Phys. Rev. **99**, 621 (1955).

[10] Taylor, Lönsjö, and Bonner, Phys. Rev. **100**, 174 (1955).

[11] Bethe, Beyster, and Carter, Los Alamos Scientific Laboratory Report LA-1429, 1955 (unpublished).

2.5-Mev Measurements.—Neutrons of 2.5 Mev were produced by bombarding a tritium-gas target with monoenergetic protons from an electrostatic accelerator. The gas target was 6.0 cm in length and contained tritium at an absolute pressure of 60 cm Hg. The target chamber was separated from the accelerating tube vacuum system by a 0.001-cm-thick molybdenum foil. The over-all energy spread of the neutrons was about 200 kev, the factors determining this spread being the thickness of the tritium-gas target and the straggling of protons through the molybdenum foil. Throughout the experiment, proton beams of 4 to 5 μa were used.

The neutrons were detected by a cylindrical, methane-filled, proportional counter having a 0.0025-cm center wire surrounded by a 2.0-cm-diameter outer wall. The counter was operated at 10 atmos of purified methane and with 1500 volts on the center wire. Pulses produced by proton recoils in the counter were amplified by three amplifiers operated in parallel, with the output of each amplifier going to two scalers. The discriminator bias of each of the six scalers was set at one of three values; the two disciminators operating at the same bias being fed by different amplifiers. Thus, data were taken simultaneously at three energy thresholds, and scaling errors and shifts in amplification could be recognized quickly by differences in the counting rates of the two scalers operating at the same bias. The three biases were set to give detection thresholds at about 2.0, 1.6, and 1.2 Mev.

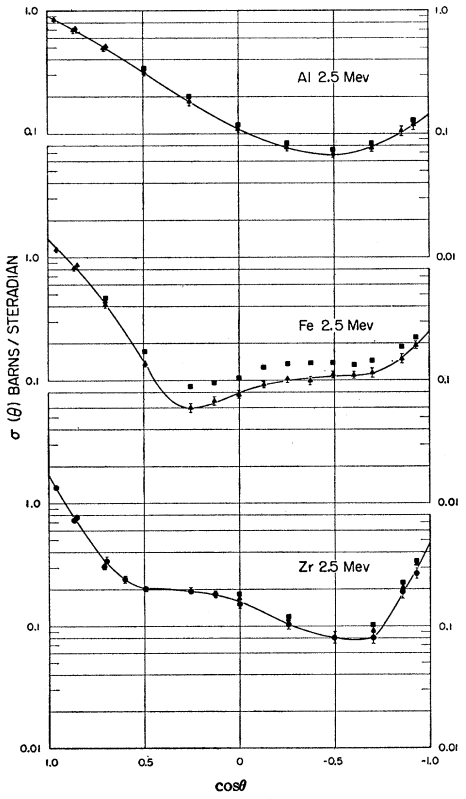

FIG. 2. Differential cross section in the laboratory system for elastic scattering of 2.5-Mev neutrons by Al, Fe, and Zr. The circles, triangles, and squares denote data taken with the detector biased at 2.0, 1.6, and 1.2 Mev, respectively.

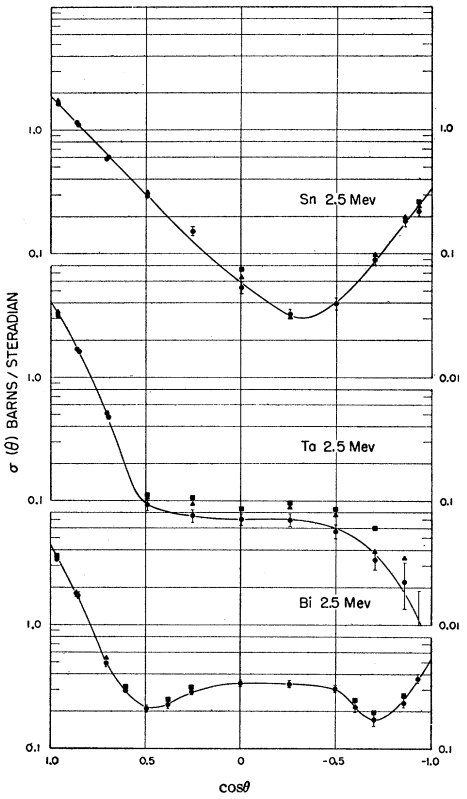

FIG. 3. Differential cross sections in the laboratory system for elastic scattering of 2.5-Mev neutrons by Sn, Ta, and Bi. The circles, triangles, and squares denote data taken with the detector biased at 2.0, 1.6, and 1.2 Mev, respectively.

The energy sensitivity of the detector was measured by observing at various neutron energies the ratio of the counting rate of the recoil counter to the counting rate of a "long counter"[12] whose response had been calibrated by comparison with a neutron counter telescope of known energy dependence.[13]

Polyethylene wedges shielded the counter from the neutron source.

7.0-Mev Measurements.—The measurements at 7.0 Mev were made with neutrons produced by the D(d,n)He^3 reaction. Deuterium gas at a pressure of 120 cm Hg was contained in a target system identical to that described above. The spread in neutron energy was about 400 kev, again being due to the thickness of the gas target and straggling in the molybdenum foil. Deuteron beams of about 4 μa were used throughout the experiment. A scintillation counter similar to that

[12] A. O. Hanson and J. L. McKibben, Phys. Rev. **72**, 673 (1947); Nobles, Day, Henkel, Jarvis, Kutarnia, McKibben, Perry, and Smith, Rev. Sci. Instr. **25**, 334 (1954).

[13] C. H. Johnson and C. C. Trail, Rev. Sci. Instr. (to be published); Bame, Haddad, Perry, and R. K. Smith, Rev. Sci. Instr. (to be published).

described elsewhere[14] was used to detect the scattered neutrons. The phosphor consisted of four 0.5-cm-diameter plastic phosphor spheres which were separated from each other by about 1.5 cm of Dow Corning 200 grease. Most of the data were taken with an energy threshold set at about 80% of the energy of the elastically scattered neutrons. Hence, during measurements of scattering from light elements, the threshold was lowered as the scattering angle increased. Copper wedges were used to shield the counter from the neutron source. The energy sensitivity of the detector was determined in the manner described in the 2.5-Mev part of this experiment.

B. Measurements of Inelastic Collision Cross Sections

The inelastic collision cross section, which is the cross section for all processes other than elastic scattering, was obtained by two different methods: (1) by subtracting the elastic cross sections from the total cross sections and (2) by the sphere transmission technique. To obtain inelastic cross sections by the first method, the measured differential cross section for elastic scattering was integrated over 4π steradians to obtain the elastic cross section, and this result was subtracted from a measured total cross section. The experimental techniques used to measure differential elastic cross sections are discussed in Sec. IIA, and the method of measuring total cross sections is described in Sec. IIC.

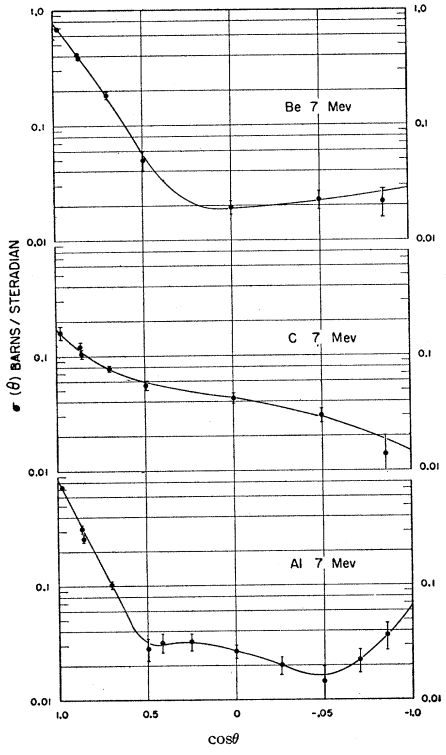

FIG. 4. Differential cross sections in the laboratory system for elastic scattering of 7.0-Mev neutrons by Be, C, and Al. The points indicate the results obtained with a detection threshold of about 80% of the energy of the elastically scattered neutrons.

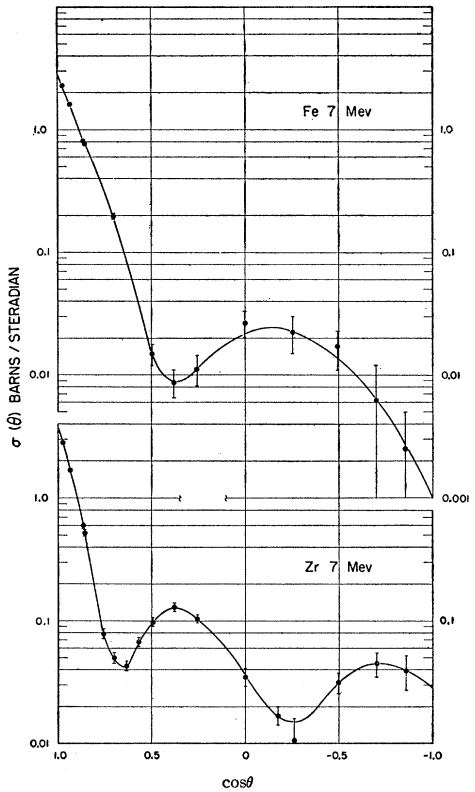

FIG. 5. Differential cross sections in the laboratory system for elastic scattering of 7.0-Mev neutrons by Fe and Zr. The points indicate the results obtained with a detection threshold of 80% of the energy of the elastically scattered neutrons.

The sphere transmission technique has been explained in detail in previous publications[11,15] and will be reviewed only briefly in this report. The transmission of a spherical shell of material is measured by observing the ratio of the counting rate of an energy-sensitive neutron detector surrounded by the sphere to the counting rate of the detector with sphere removed. The neutron detector is biased to discriminate against neutrons which have been inelastically scattered in the sphere. The sphere transmission is primarily a measure of the inelastic scattering cross section because the elastic scattering into the neutron detector by the sphere tends to compensate for the elastic scattering of neutrons out of the direct flux between source and detector. The first-order cancellation of elastic scattering is the advantage of the sphere method and is especially helpful when the inelastic cross section to be measured is a small fraction of the total cross section. The neutron detector can be biased at many energy thresholds to give a qualitative

[14] McCrary, Taylor, and Bonner, Phys. Rev. 94, 808 (1954).

[15] Beyster, Henkel, Nobles, and Kister, Phys. Rev. 98, 1216 (1955).

picture of the energy spectrum of inelastic scattering. This information is also useful in determining whether the detector is counting neutrons from inelastic scattering at the higher-energy thresholds used in the experiment.

In order to measure inelastic collision cross sections accurately by the sphere technique, corrections must be evaluated for several effects: (1) multiple elastic collisions in the sphere, (2) variation of the intensity and energy of the neutron source over the solid angle subtended by the sphere, (3) finite size of the neutron detector, and (4) energy loss on elastic collisions. In many situations this last effect necessitates the most significant correction to the data. The detailed methods of making all of these corrections are discussed in previous papers.[11,15] Cross-section information used in the corrections to the observed data includes the total neutron cross sections and the angular distributions for elastic scattering. Information on total cross sections available in compilations[16] is adequate for these corrections since the inelastic collision cross sections deduced from the analysis are not very sensitive to the total cross section used. Angular distributions for elastic scattering for many elements and energies are also available now from this investigation and from recently published reports.[6–9] When a direct measurement of an angular distribution is not available, it can be estimated with sufficient accuracy for any element with atomic weight of 27 or more at neutron energies between 1 Mev and 14 Mev. At present the precision of the sphere experiment is as much limited by the counting statistics and reproducibility as by uncertainties in making the corrections to the experimental measurements. The four corrections discussed above were made analytically on the MANIAC computer for each element at each energy and detector bias by the procedure given in reference 15.

1.0-, 1.77-, 2.5-, and 3.25-Mev Measurements.—These sphere transmission experiments were done with the electrostatic accelerator using the $T(p,n)He^3$ neutron source reaction. The gas target was 6.0 cm long and was filled with tritium to a pressure of 40 cm Hg. The analyzed proton beam passed through a 0.0005-cm-thick aluminum window into the target chamber. The over-all energy spread of the neutron source was about 80 kev, which was generally sufficient to average over many resonances in the compound nucleus.

The gas proportional counter described in reference 15 was used again here. This detector was filled to 8.5 atmos with a gas mixture of 70% krypton and 30% methane and was biased at eight energy thresholds. The angular dependence of the detector sensitivity was minimized by adjusting the gas multiplication in the detector. The variation of detector efficiency with counting rate was investigated over a large range of neutron fluxes, and no undesirable effects were observed. However, the counting rate of this detector was quite sensitive to temperature, necessitating the control of both room and sphere temperature.

A shadow shield was placed between source and detector to determine the effect of room background on the observations. Sphere transmissions were then measured for these background neutrons. The effect of this room background on the measured sphere transmissions was 0.1% or less. The effect of background arising from neutrons produced by reactions other than the source reaction was measured by removing the tritium from the gas target chamber and again measuring the sphere transmission. The effect of this background on the measured sphere transmission was also less than 0.1%. Thus no correction for background was necessary to the measured transmissions.

A stabilized system of electronics consisting of amplifiers, discriminators and scalers in parallel was used since high precision was desired in the transmission measurements. In addition, many individual transmission measurements were made at short time intervals to eliminate the effects of long-term drifts in the detector or electronics. A current integrator that ended the run when a predetermined proton charge had been

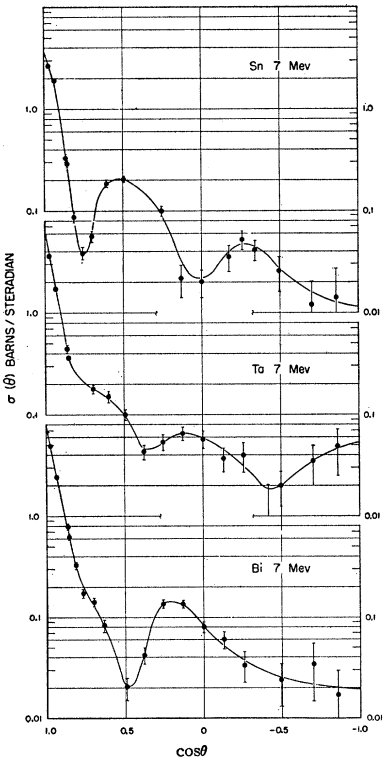

FIG. 6. Differential cross sections in the laboratory system for elastic scattering of 7.0-Mev neutrons by Sn, Ta, and Bi. The points indicate the results obtained with detection threshold of 80% of the energy of the elastically scattered neutrons.

[16] D. J. Hughes and J. A. Harvey, *Neutron Cross Sections*, Brookhaven National Laboratory Report BNL-325 (Superintendent of Documents, U. S. Government Printing Office, Washington, D. C., 1955).

TABLE I. Inelastic cross sections for 1-Mev neutrons (barns).

Element	Inelastic collision cross section	Energy threshold (kev) 800	700	600	500	400
Ti	0.17±0.07	0.17±0.07	0.16	0.15	0.15	0.15
Fe	0.49±0.06	0.54±0.10	0.52	0.51	0.50	0.49
Ni	0.06±0.03	−0.01±0.06	0.03	0.05	0.06	0.06
Zr	0.13±0.04	0.15±0.07	0.15	0.14	0.14	0.13
Ag	1.72±0.20	1.60±0.10	1.49	1.38	1.25	1.10
Cd	1.04±0.07	1.04±0.07	1.03	0.98	0.92	0.88
W	2.25±0.30	1.65±0.20	1.15	0.93	0.74	0.58
Au	1.75±0.20	1.63±0.10	1.52	1.36	1.18	1.03
U(normal)	1.80±0.25	1.55±0.20	1.35	1.20	1.00	0.90
U^{235}	2.70±0.30	2.63±0.27	2.57	2.50	2.44	2.35

collected at the target was the primary monitor in this experiment. A "long counter," which gave an indication of the total source yield, was used as an auxiliary monitor.

TABLE II. Inelastic cross sections for 1.77-Mev neutrons (barns).

Element	Inelastic collision cross section	Energy threshold (Mev) 1.40	1.23	1.05	0.88
Al	0.15±0.03	0.12±0.09	0.15	0.15	0.15
Ti	0.55±0.05	0.55±0.06	0.55	0.55	0.55
Fe	0.73±0.04	0.74±0.06	0.73	0.69	0.55
Zr	0.60±0.05	0.61±0.06	0.61	0.58	0.53
Cd	1.55±0.10	1.55±0.11	1.55	1.40	1.10
Sn	0.72±0.04	0.72±0.07	0.73	0.72	0.69
Au	2.20±0.17	2.12±0.13	2.00	1.75	1.40
Bi	0.40±0.04	0.41±0.07	0.41	0.39	0.32

The relative energy sensitivity of the neutron detector was necessary for the correction for energy loss on elastic collisions. This quantity was determined by measuring the ratio of the counting rate at the various neutron energies to the counting rate at the neutron energy used in the transmission experiment. Corrections for changes in neutron flux with energy were made from the known $T(p,n)He^3$ zero-degree absolute yields.[17] The angular intensity of the neutron source, which must be known to correct for flux variations over the surface of the sphere, was measured by placing the neutron detector at various small angles with respect to the forward direction, and determining at each bias the ratio of the counting rate at a given angle to that at zero degrees.

7.0-Mev Measurements.—The $D(d,n)He^3$ neutron source referred to in Sec. IIA was also used here. The 7.0-Mev experiment was done with a detector of the type used in the 4.0-Mev experiments reported in reference 15. A sphere of hydrogenous plastic phosphor 0.7 cm in diameter was mounted on a 12-cm quartz light pipe which was cemented to a 6467 DuMont photomultiplier. This proton-recoil detector was biased to have detection thresholds at several neutron energies between 3.5 and 6.0 Mev. A photomultiplier tube was selected which did not show significant gain changes with counting rate variations. The efficiency of the detector for the 2.6-Mev gamma rays from ThC″ was only a few percent of the crystal's efficiency for 7.0-Mev neutrons at the lowest bias. The detection efficiency for 6.2-Mev gamma rays was investigated using the $F^{19}(p,\alpha\gamma)O^{16}$ reaction,[18] and it was apparent from these measurements that high-energy gamma radiation could influence the results of the sphere experiments at the lower thresholds. However, cross-section determinations at the higher detector thresholds were not affected. Therefore, the observed decrease of inelastic cross section in Table V as the threshold is lowered may not be entirely due to the detection of inelastically scattered neutrons but may be partly due to high-energy gamma rays produced by inelastic scattering in the sphere.

TABLE III. Inelastic cross sections for 2.5-Mev neutrons (barns).

Element	Inelastic collision cross section	Sphere experiment Energy thresholds (Mev) 2.0	1.75	1.50	1.25	1.00	$\sigma_t-\sigma_{el}$ experiment 2.0 Mev
C	0.05±0.05	0.01±0.11	0.03	0.04	0.05	0.05	···
Al	0.38±0.05	0.38±0.08	0.38	0.38	0.38	0.37	0.41±0.16
Ti	0.79±0.06	0.79±0.06	0.79	0.78	0.73	0.61	···
Fe	1.04±0.05	1.04±0.07	1.04	0.97	0.73	0.61	0.91±0.15
Ni	0.80±0.06	0.80±0.10	0.80	0.80	0.79	0.77	···
Cu	1.27±0.06	1.27±0.09	1.25	1.20	1.12	1.05	···
Zn	1.30±0.10	1.30±0.09	1.27	1.20	1.08	0.95	···
Zr	1.16±0.06	1.17±0.08	1.17	1.15	1.11	1.05	1.25±0.16
Ag	2.08±0.12	2.07±0.12	1.99	1.88	1.82	1.81	···
Cd	1.92±0.12	1.92±0.12	1.88	1.80	1.67	1.58	···
Sn	1.37±0.07	1.39±0.10	1.37	1.35	1.31	1.24	1.14±0.25
Ta	2.90±0.35	···	···	···	···	···	2.89±0.25
W	2.66±0.30	2.64±0.27	2.59	2.50	2.38	2.29	···
Au	2.72±0.20	2.67±0.16	2.61	2.54	2.45	2.38	···
Pb	0.71±0.06	0.71±0.07	0.71	0.65	0.54	0.49	···
Bi	0.75±0.06	0.76±0.08	0.73	0.66	0.56	0.48	0.42±0.35
U(normal)	3.20±0.30	3.15±0.25	3.00	2.70	2.50	···	3.10±0.30
U^{235}	3.25±0.30	3.20±0.27	3.20	3.12	2.95	2.75	···

[17] Haddad, Henkel, Perry, and Smith (unpublished).
[18] Streib, Fowler, and Lauritsen, Phys. Rev. **59**, 253 (1941); R. B. Day and R. L. Walker, Phys. Rev. **85**, 582 (1952).

The response of this detector to neutrons entering at various angles was constant to within 2% over 90% of the solid angle; hence no correction for detection asymmetry was necessary. However the efficiency of the detector was a function of temperature so that it was necessary to control the temperature of the room and spheres. Again many short runs were involved in a transmission determination to average out long-term drifts.

Room and target backgrounds were found to be small and no corrections to the experimental data were necessary. The angular intensity of the neutron source and the energy sensitivity of the detector were measured by the methods given in the discussion of the lower-energy sphere experiments.

C. Total Cross Sections

In the analysis of the measurements of differential cross sections for elastic scattering and of inelastic collision cross sections, it was necessary to know total neutron cross sections. These total cross sections were obtained by observing the transmission of cylindrical samples. The neutron sources described in Sec. IIA were also used in the transmission measurements. A scintillation detector containing a cylindrical stilbene phosphor 1 cm in length by 1 cm in diameter detected the neutrons. This detector was operated at two biases set at about 75% and 40% of the maximum pulse height. The source-to-detector distance was 85 cm for the measurements at 2.5 Mev and 115 cm for those at 7 Mev. Backgrounds, which were measured by inserting a copper bar 40 cm in length between the neutron source and counter, were less than 2% of the direct counting rate. The transmission samples were cylinders 2.5 cm in diameter and of a length necessary to give transmissions of about 0.6. The samples were placed midway between the neutron source and detector. Using the differential cross sections for scattering at small angles obtained in the angular-distribution measurements, small corrections were made for the scattering of neutrons into the detector by the scattering samples. The cross sections obtained at the two biases agreed to within 0.5%.

TABLE IV. Inelastic cross sections for 3.25-Mev neutrons (barns).

Element	Inelastic collision cross section	Energy thresholds (Mev) 2.60	2.28	1.95	1.63	1.30
Al	0.53±0.05	0.53±0.05	0.53	0.52	0.48	0.42
Ti	0.98±0.07	0.98±0.07	0.97	0.91	0.81	0.66
Fe	1.09±0.07	1.09±0.07	1.08	0.96	0.83	0.71
Zr	1.44±0.08	1.44±0.09	1.44	1.43	1.40	1.33
Cd	1.95±0.12	1.95±0.12	1.94	1.91	1.82	1.73
Sn	1.73±0.09	1.73±0.10	1.73	1.72	1.65	1.54
Au	2.63±0.15	2.59±0.13	2.57	2.54	2.50	2.43
Bi	1.33±0.07	1.33±0.10	1.31	1.25	1.11	1.00

III. RESULTS

A. Differential Cross Sections for Elastic Scattering

The differential cross sections for elastic scattering of 2.5-Mev neutrons by Al, Fe, Zr, Sn, Ta, and Bi, are shown in Figs. 2 and 3. The circles, triangles, and squares denote data taken with the detector biased at thresholds of 2.0, 1.6, and 1.2 Mev, respectively. For Al and Fe the data taken with the 2.0-Mev threshold required large corrections for the energy loss in elastic collisions and were therefore more uncertain than the data taken with the 1.6-Mev threshold. Since no inelastic scattering occurs in which the neutrons lose less than about 0.85 Mev in Al and Fe, the medium-bias

TABLE V. Inelastic cross sections for 7.0-Mev neutrons (barns).

Element	Inelastic collision cross section	Sphere experiment Energy thresholds (Mev) 5.6	4.9	4.2	$\sigma_t-\sigma_{el}$ experiment 5.6 Mev
Be	0.60±0.04	0.58±0.06	0.59	0.60	0.55±0.06
C	0.17±0.03	0.16±0.04	0.17	0.14	0.15±0.04
Al	0.86±0.05	0.86±0.06	0.85	0.74	0.89±0.05
S	1.14±0.07	1.14±0.11	1.14	1.08	···
KCl	1.12±0.11	1.12±0.11	1.09	1.01	···
Ca	1.14±0.07	1.14±0.11	1.13	1.06	···
Ti	1.30±0.06	1.30±0.07	1.28	1.10	···
Fe	1.41±0.07	1.41±0.07	1.39	1.30	1.41±0.11
Ni	1.48±0.06	1.48±0.10	1.48	1.37	···
Cu	1.54±0.06	1.54±0.08	1.52	1.35	···
Zn	1.61±0.10	1.61±0.10	1.58	1.45	···
Zr	1.70±0.08	1.70±0.09	1.69	1.65	1.75±0.12
Ag	2.00±0.10	1.98±0.10	1.93	1.74	···
Cd	2.05±0.10	2.04±0.10	1.94	1.78	···
Sn	2.00±0.10	1.99±0.12	1.93	1.79	1.98±0.11
Ta	2.50±0.20	···	···	···	2.49±0.14
W	2.45±0.20	2.43±0.17	2.39	2.15	···
Au	2.50±0.15	2.49±0.13	2.45	2.32	···
Pb	2.38±0.15	2.38±0.15	2.36	2.28	···
Bi	2.38±0.14	2.38±0.14	2.36	2.19	2.46±0.20

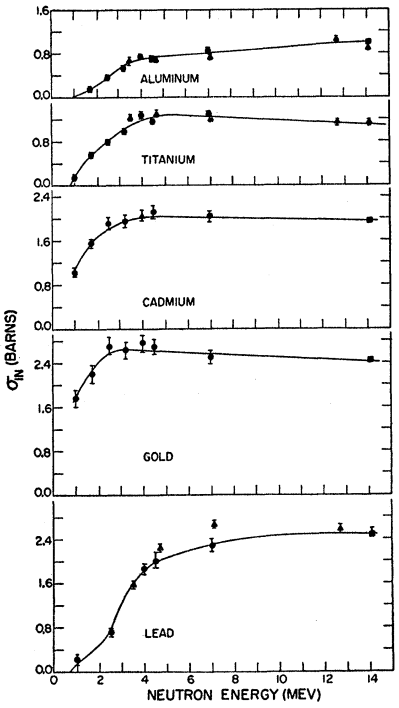

FIG. 7. Inelastic collision cross sections at various neutron energies for Al, Ti, Cd, Au, and Pb. The circles denote the results of this report and references 2 and 15, the triangle values of Taylor *et al.*,[10] and the squares the work of Graves and Davis.[24]

data give reliable values for the elastic differential cross sections for these two elements.

The results of the differential cross-section measurements at 7.0 Mev are shown in Figs. 4, 5, and 6. The points indicate the results obtained with detection thresholds of about 80% of the energy of elastically scattered neutrons. The threshold, therefore, depends upon the atomic weight of the scattering sample and upon the scattering angle, the threshold being 3.5 Mev for the measurement of Be at 150°. For some of the elements the statistical errors were too large to define accurately the shape of the differential cross-section curves. In these cases considerable weight in drawing the curves was given to the information obtained at lower biases where the statistical accuracy was much improved, although the absolute value of the cross section was increased by the presence of inelastically scattered neutrons. The errors indicated on the experimental points contain the uncertainties in the counting statistics, the multiple-scattering correction, the angular-resolution correction, the scatterer-to-counter distance, and the energy sensitivity of the detector. The possible errors in the multiple-scattering correction and the angular-resolution correction were estimated to be 25% of the magnitude of the correction.

B. Inelastic Collision Cross Sections

Inelastic cross sections measured at 1.0-, 1.77-, 2.5-, 3.25-, and 7.0-Mev neutron energies are given in Tables I, II, III, IV, and V, respectively. Results from the sphere method and the elastic-scattering method are both tabulated. Estimates of the inelastic collision cross sections are given in the first column. These values are based on measurements at the lower energy thresholds when available data indicate that no neutrons from inelastic scattering are detected at these thresholds. The second column gives the inelastic cross sections deduced from the sphere experiment at an energy threshold of 80% of the incident neutron energy. In succeeding columns the cross sections at several lower-energy thresholds are given to indicate the magnitude of the inelastic scattering to neutron energies below each threshold. In the last columns of Tables III and V are tabulated inelastic collision cross sections determined by subtracting the measured elastic scattering cross section from the measured total cross section. These results were obtained at a threshold of about 80% of the incident neutron energy.

Inelastic collision cross sections for 1.0-Mev neutrons have been reported previously for some of the elements listed in Table I. The former measurements were made with a neutron source having a total energy spread of 160 kev while the present work was done with an 80-kev energy spread. In general the two sets of determinations agree to within experimental uncertainties. However a variation of the order of experimental error should exist in the case of the iron data because the present and former cross sections are different averages over the resonance structure in the inelastic cross section of iron at 1.0 Mev.

For the sphere experiment the errors are given for both the cross sections measured at the 80% threshold and for the inelastic collision cross sections. The uncertainties in the following quantities were considered: (1) the measurement of sphere transmission, (2) the variation of the neutron source intensity with angle, (3) the energy sensitivity of the neutron detector, (4) the auxiliary cross sections used in the multiple scattering analysis (the total cross section and the differential cross section for elastic scattering), and (5) the correction for energy losses in elastic collisions. The uncertainty in the inelastic collision cross section is often less than the uncertainty in the cross section measured at the 80% threshold because the inelastic collision cross section is based on measurements at the lower detector thresholds when no neutrons from inelastic scattering are detected. Experimental uncertainties are given in the last column for the inelastic collision cross sections determined by subtracting the elastic cross sections from the total cross sections. These errors are based on an uncertainty of about 5% in the elastic cross section and a 1 or 2% uncertainty in the total cross section.

The inelastic collision cross sections for several typical elements are plotted as a function of energy in Fig. 7. Similar curves for Fe, Zr, Sn, and Bi are given in the lower part of Figs. 8, 9, 10, and 11, respectively. Experimental data are now available from which

similar excitation curves may be prepared for about sixteen elements. These curves give the average variation of the inelastic collision cross section with energy since all the measured cross sections are averaged over resonances in the compound nucleus. The cross section is very small until the incident neutron energy is greater than the energy of the first excited state in the target nucleus. Above this energy the cross sections for all elements increase with energy and reach a plateau at 3 to 6 Mev. For target nuclei having wide-level spacings, as for example in bismuth, this rise is more gradual than for target nuclei with closely-spaced levels.

The inelastic collision cross sections reported here can be compared with those obtained in other experiments. With few exceptions the cross sections determined by various methods are in good agreement. For example, the results obtained by the sphere method are consistent with the results obtained by subtracting the measured elastic cross section from the measured total cross section. The cross sections determined by disk scattering experiments[19] at 1.5- and 3.0-Mev neutron energies also agree with the cross sections from the sphere transmission measurements. However, at 2.5-Mev neutron energy the inelastic cross sections measured with the sphere technique of Pasechnik[20] differ significantly from the results presented here for Al, Cu, Zn, and Pb while agreeing fairly well with these results on Fe, Ni, Ag, Cd, W, and Bi. Another disagreement exists for the inelastic cross section of zirconium. Cross sections based on measurements of de-excitation gamma rays following inelastic neutron scattering[21] are about 30% higher than the value given in Table II. A possible disagreement is also indicated at 7.0-Mev neutron energy for bismuth and lead where our inelastic cross sections are several tenths of a barn less than those of reference 10, which were obtained by the same experimental method. The values reported here at 7.0 Mev are consistent with the results of integral measurements of inelastic collision cross section at an average neutron energy of 6 Mev.[11]

IV. THEORETICAL INTERPRETATIONS

Calculations by Feshbach, Porter, and Weisskopf[1] and others[2–4] have shown that many features of the interaction of fast neutrons with nuclei can be explained by representing the neutron-nucleus interaction by a complex potential well. Such a representation gives cross sections averaged over many resonances in the compound nucleus. Using this model, one can calculate the total cross section, the differential cross section for shape-elastic scattering (the scattering process which does not proceed through an intermediate compound

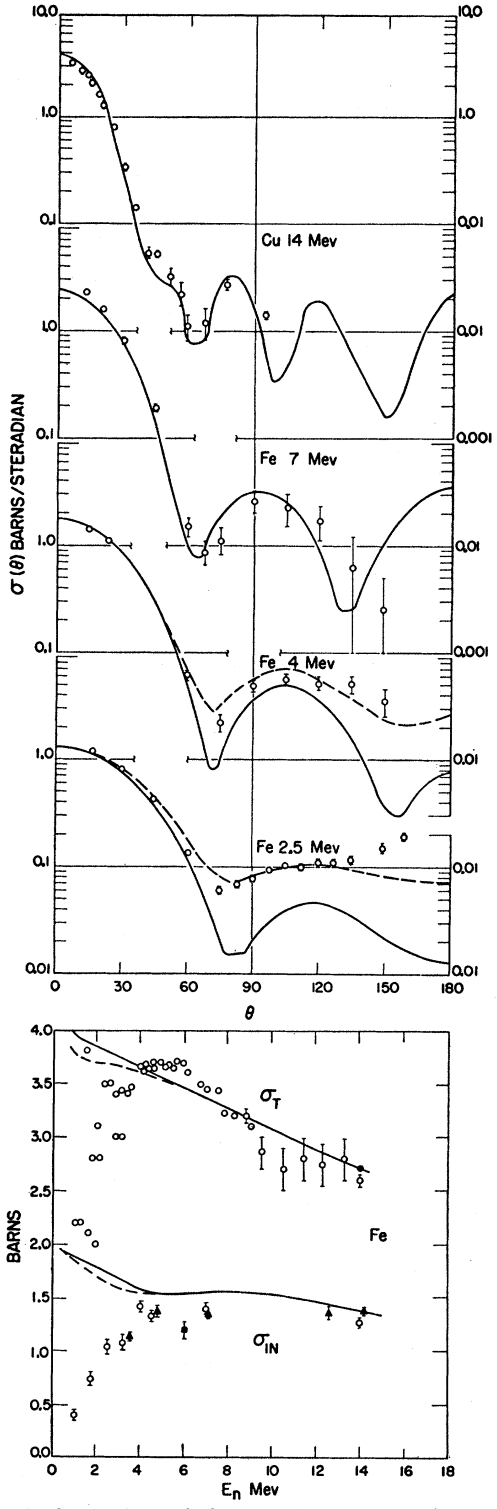

FIG. 8. Comparison of theory and experiment for iron and copper. The circles, squares, and triangles denote the experimental data. The solid curves are calculated with the energy independent parameters of Table VI. The dashed curves of differential cross sections are the sum of shape-elastic and compound-elastic scattering. The dashed curves of the total and the compound nucleus formation cross section are calculated with the energy-dependent parameters. All quantities are in the laboratory system of coordinates.

[19] P. Olum, U. S. Atomic Energy Commission Report MDDC-353, 1945 (unpublished); Barschall, Battat, Bright, Graves, Jorgensen, and Manley, Phys. Rev. **72**, 881 (1947).

[20] M. V. Pasechnik, *Proceedings of the International Conference on the Peaceful Uses of Atomic Energy, Geneva*, 1955 (United Nations Publications, New York, 1956), Vol. 2, Paper 714.

[21] J. B. Guernsey and C. Goodman, Phys. Rev. **101**, 294 (1956).

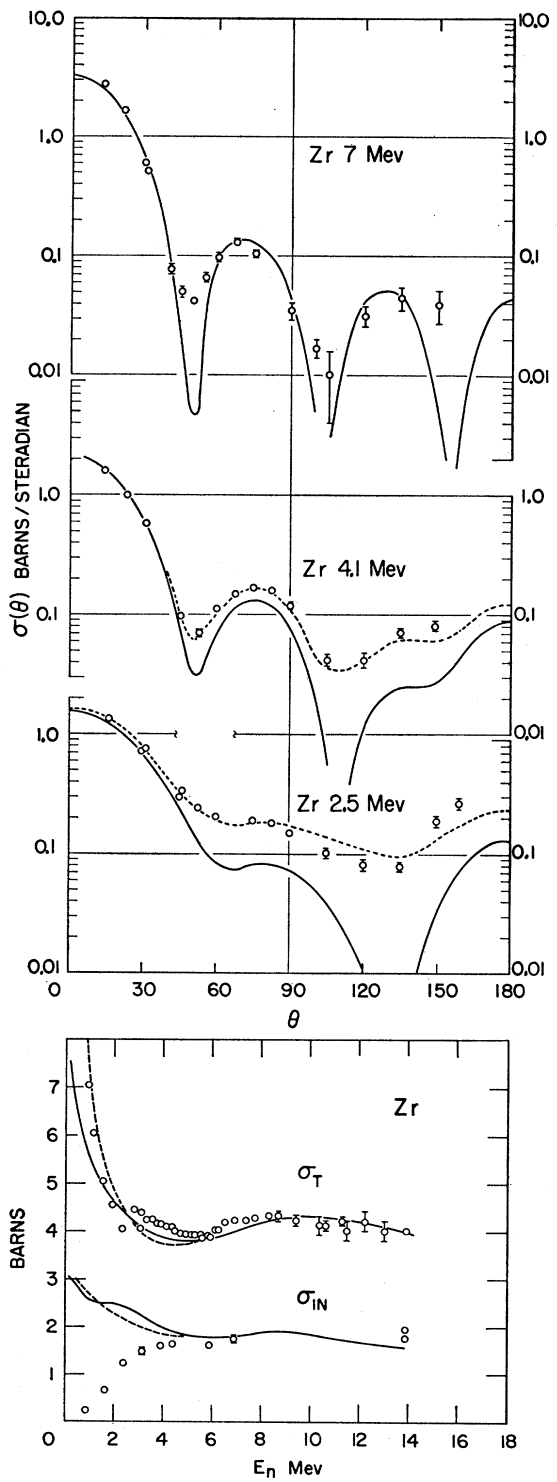

FIG. 9. Comparison of theory and experiment for zirconium. The circles are the experimental data. The solid curves are calculated with the energy independent parameters of Table VI. The dashed curves of differential cross sections are the sum of shape-elastic and compound-elastic scattering. The dashed curves of the total and the compound nucleus formation cross section are calculated with the energy-dependent parameters. All quantities are in the laboratory system of coordinates.

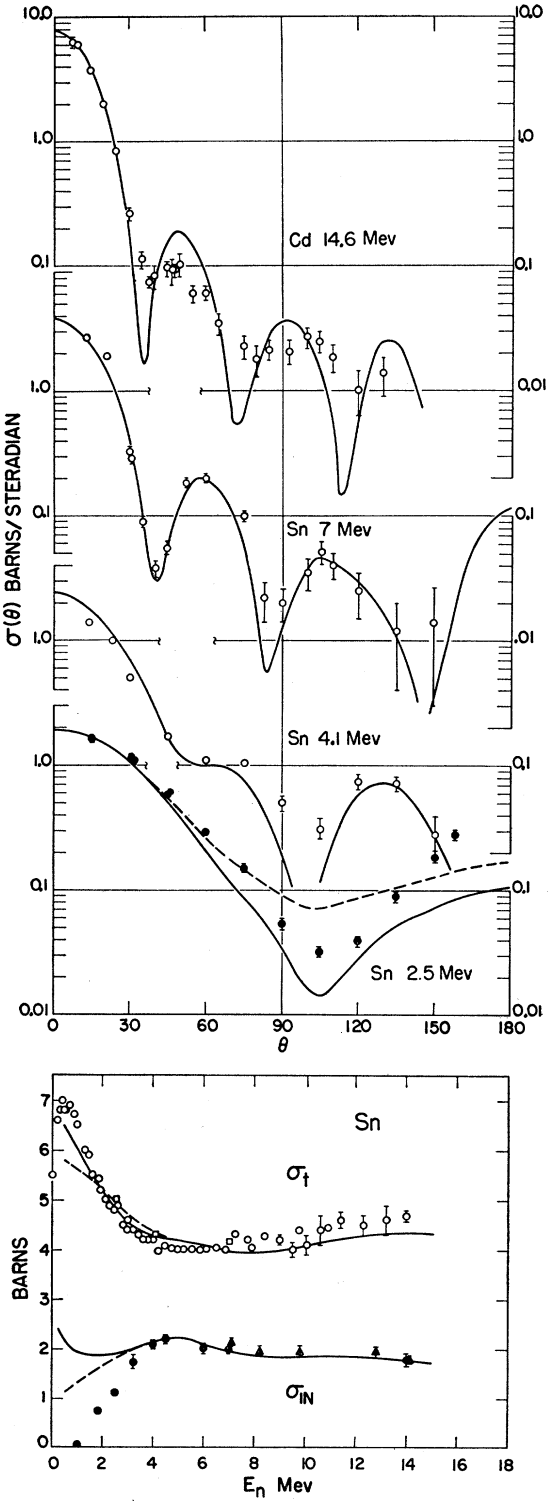

FIG. 10. Comparison of theory and experiment for tin and cadmium. The circles, squares, and triangles are the experimental data. The solid curves are calculated with the energy independent parameters of Table VI. The dashed curves of differential cross sections are the sum of shape-elastic and compound-elastic scattering. The dashed curves of the total and the compound nucleus formation cross section are calculated with the energy-dependent parameters. All quantities are in the laboratory system of coordinates.

state), and the cross section for the formation of a compound nucleus. The total cross sections obtained in this manner can be compared directly with experiment. On the other hand, the calculated values of the cross section for compound nucleus formation and the shape-elastic scattering cross section cannot, in general, be compared directly with experimental quantities. The compound nucleus may decay either by the entrance channel, giving compound-elastic scattering, or by other energetically possible channels, giving the inelastic collision (reaction) cross section. The calculated cross section for compound nucleus formation is, therefore, only an upper limit to the inelastic collision cross section. Similarly, since experiments in which elastic scattering is observed actually measure the sum of the shape-elastic and compound-elastic scattering, the experimental data do not correspond to the calculated shape-elastic scattering cross sections. At energies above several Mev, where there are many energetically possible modes of decay of the compound nucleus, compound-elastic scattering is expected to be small, and the experimental quantities will correspond more closely to the calculated ones.

Although a potential employing a square-well radial dependence is preferable from the standpoint of calculational simplicity to potentials with more involved shapes, it was found in previous work[1,2] that cross sections for compound nucleus formation obtained from the square-well potential were significantly smaller than the experimental values of the inelastic collision cross sections. Since one of the most unrealistic aspects of the model was the sharp edge of the square well, it seemed reasonable to modify the model to include a smooth radial dependence. A diffuse-edge nuclear potential that has been used successfully by Woods and Saxon[5] to explain proton scattering results was chosen. For an element of atomic weight A the potential is given by

$$V(r)=\frac{V_0(1+i\zeta)}{1+\exp[(r-R)/a]}, \tag{1}$$

where

$$R=r_0A^{\frac{1}{3}}\times10^{-13}\text{ cm}.$$

This potential contains four parameters, a well depth V_0, an absorption parameter ζ, a radius r_0, and a diffuseness a.

Elements for which considerable experimental information was available were selected, and attempts were made to obtain agreement between experiment and theory by adjusting the four parameters independently. The experimental data include the differential cross sections for elastic scattering of 1.0-, 2.5-, 4.1-, 7.0-, and 14.0-Mev neutrons and the total cross sections and inelastic collision cross sections for energies up to 14 Mev. The parameters were allowed to vary from element to element but, in the first attempt to fit the data, were required to be energy-independent. It was found that considerable latitude exists in the choice

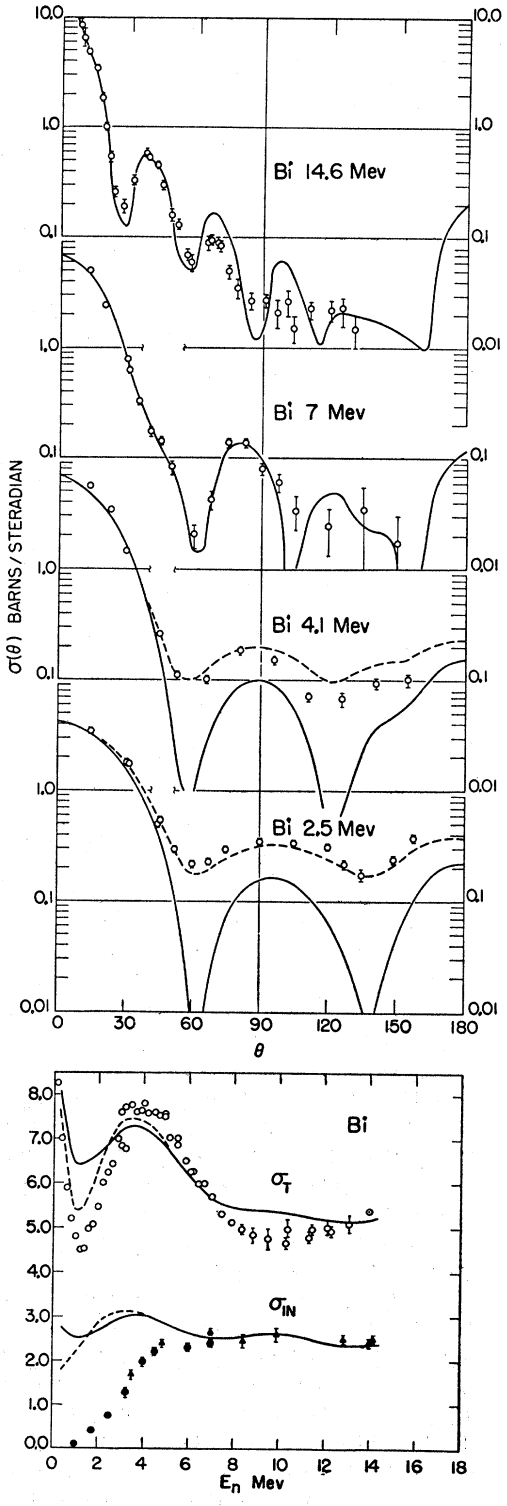

FIG. 11. Comparison of theory and experiment for bismuth. The circles, squares, and triangles are the experimental data. The solid curves are calculated with the energy-independent parameters of Table VI. The dashed curves of differential cross sections are the sum of shape-elastic and compound-elastic scattering. The dashed curves of the total and the compound nucleus formation cross section are calculated with the energy-dependent parameters. All quantities are in the laboratory system of coordinates.

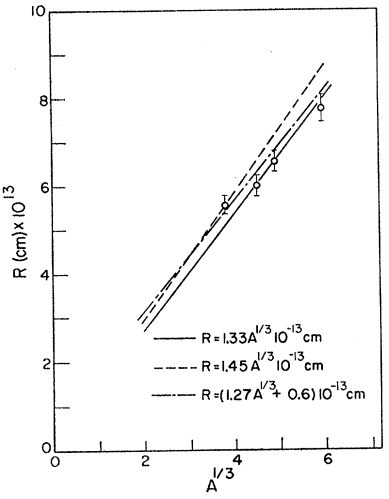

FIG. 12. Variation of nuclear radius with atomic weight, determined by fitting cross sections calculated on the basis of Eq. (1) with experimental measurements.

of parameters which satisfy the experimental data on any one element at one neutron energy. For example, the nuclear radius can often be varied as much as 15% if the potential V_0 is also allowed to vary. The requirement that the parameters be energy independent, or nearly so, limits the choice of acceptable parameters. The calculations show that essentially all experimental features can be accounted for by the potential of Eq. (1), using energy-independent parameters, although in some cases the quantitative agreement is not good. By allowing the absorption parameter to increase with increasing energy and the well depth V_0 to decrease slightly with increasing neutron energy, significantly better fits were obtained for some of the heavier elements. In particular, the minimum at about 1 Mev in the total cross section of the heavy elements cannot be reproduced accurately unless the absorption parameter is allowed to increase with energy.

In Figs. 8 to 11 comparison is made between the experimental and theoretical cross sections. The angular distributions at 14 Mev are the data of Cross[9] and of Coon.[8] The differential cross sections at all other energies are from this paper or from reference 2. The total cross sections below 3 Mev are taken from Miller *et al.*[22]; above 3 Mev the data are those of Nereson and Darden.[23] The inelastic collision cross sections were obtained from Taylor *et al.*,[10] Beyster *et al.*,[15] Graves and Davis,[24] and this paper. In all figures experimental points with their associated errors are given, and the lines give values calculated from the potential of Eq. (1). With the exception of the dashed lines in the total and inelastic collision cross-section graphs, all curves were computed using the energy-independent parameters given in Table VI. In the figures showing the inelastic collision cross sections, the lines represent the cross section for compound nucleus formation, which is the theoretical upper limit to the measured inelastic collision cross section. At low energies where the compound nucleus formation exceeds the inelastic collision cross section compound elastic scattering occurs. Hence, on the differential cross-section figures at low energies two theoretical curves are drawn. The solid curve indicates shape-elastic scattering, and the dashed curve is obtained by adding to the solid curve an isotropically distributed component of compound-elastic scattering equal in magnitude to the difference between the calculated compound nucleus formation cross section shown by the solid curve and the experimental inelastic collision cross section.

From Fig. 11 it appears that the energy-independent parameters which fit the data above about 4 Mev will not reproduce the minimum in the total cross section near 1 Mev for bismuth and that some variation of the parameters with energy is necessary. The dashed lines for total cross section and for compound nucleus formation are obtained by allowing the absorption parameter ζ and the well depth V_0 to change with energy. The absorption parameter is decreased smoothly with decreasing energy from the value of Table VI at 5 Mev to about three-quarters the Table VI value at 2.0 Mev and to one-half the Table VI value at 0.5 Mev. The well depth V_0 is increased by about 5% in going from the value of Table VI at 5 Mev to 0.5 Mev.

The fits to the differential cross-section curves shown in Figs. 8 to 11 are not appreciably affected by using the energy-dependent parameters instead of those of Table VI. The differences in the two sets of parameters are not large except at low energies where large compound elastic scattering prevents detailed comparison between theory and experiment. The differential cross sections at 1 Mev are somewhat better fitted by the energy-dependent parameters although again the large amount of compound-elastic scattering makes comparison difficult.

The angular distribution of neutrons from compound-elastic scattering is probably not isotropic although the degree of anisotropy is uncertain. Exact calculations of compound elastic scattering cannot be made from the assumption of the potential of Eq. (1) and further assumptions concerning the compound state are therefore necessary. Calculations based upon the statistical assumption result in distributions which are symmetric about 90°, the anisotropy decreasing with increasing spin of the target nucleus. Failure of the statistical assumption leads to angular distributions for compound-elastic scattering which are not symmetric about 90°. In any case the compound-elastic scattering is much more isotropic than is the shape-elastic scattering, and a 10 to 20% anisotropy does not significantly affect the comparison shown in Figs. 8 to 11. However, because of this uncertainty in the distribution of compound

[22] Miller, Adair, Bockelman, and Darden, Phys. Rev. **88**, 83 (1952).
[23] N. Nereson and S. E. Darden, Phys. Rev. **89**, 775 (1953); **94**, 1678 (1954).
[24] E. R. Graves and R. W. Davis, Phys. Rev. **97**, 1205 (1955).

elastic scattering, comparison of theoretical and experimental differential cross-section curves at energies of 4 Mev and below should be limited to the general shapes of the curves, and not too much emphasis should be placed on reproducing absolute values. It is interesting to note that in this analysis compound-elastic scattering occurs with appreciable cross section at energies as high as 4 Mev for Fe, Zr, and Bi.

The agreement between experiment and theory for iron is significantly worse than for the heavier elements. The total cross section especially seems to be very poorly fit below 3-Mev neutron energy. It is not possible to improve this fit significantly by allowing only V_0 and ζ to change with energy. However, by decreasing the nuclear radius by several percent, an improved fit to the low-energy data is possible. This inability to fit all the iron data with a single nuclear radius may be due to the fact that the level spacing of iron is so large that the measured cross sections are not properly averaged over many resonances.

A comparison of the radii which best fit the experimental data for different elements leads to a relation between nuclear radius and atomic weight. Figure 12 gives a plot of the nuclear radius as a function of the cube root of the atomic weight. The circles give values of the radii which fit the experimental data for Fe, Zr, Sn, and Bi. The curves are obtained from three expressions commonly used to calculate nuclear radii. These results indicate that the relation $R=(1.27A^{\frac{1}{3}}+0.6)\times10^{-13}$ cm does fit the data somewhat better than the other two expressions. However, due to the large latitude in the choice of radius for each element, the numerical constants in the above expression are not well defined. In particular, the radius of iron is subject to question since the fits to the experimental data are not good.

The values of the parameters found here have been compared to those found by other investigators. Woods and Saxon[5] have made similar calculations using proton scattering data at energies ranging from 5.25 to 31.5 Mev. Although they report similar variations in V_0 and ζ with energy, the values of V_0 and ζ which best fit the proton data are significantly different from those which fit the neutron data at the same bombarding energy. The value of V_0 for protons is from 5 to 10 Mev greater than the values for neutrons of the same incident energy and the value of ζ which fits the 5.25-Mev proton data is 0.017, a factor of about 5 less than the value necessary for neutron scattering data. The difference in the value of V_0 for neutrons and protons can be explained by the Coulomb forces affecting the proton in the nuclear well.

TABLE VI. Energy-independent parameters for Eq. (1) which give reasonable agreement between theory and experiment.

	$R\times10^{+13}$ cm	V_0(Mev)	ζ	a
Fe	5.55±0.20	39±5	0.2 ±0.05	0.35±0.10
Zr	5.99±0.25	45±5	0.1 ±0.04	0.5 ±0.10
Sn	6.62±0.25	46±5	0.1 ±0.04	0.4 ±0.10
Bi	7.72±0.30	44±5	0.075±0.03	0.5 ±0.10

From the foregoing discussion several conclusions can be drawn. The complex well representation of the nucleus appears to give a reasonable description of the interaction of fast neutrons with nuclei. Although additional mechanisms, such as spin-orbit forces and direct interactions, must be present to account for the polarization upon scattering and for the spectra of inelastically scattered neutrons,[25] cross-section calculations can be made to a good approximation without the inclusion of these features. The theory may be used to predict values of the total cross section at all energies and the differential elastic cross sections and inelastic collision cross sections above neutron energies at which appreciable compound elastic scattering occurs. The introduction of a diffuse well has removed an outstanding difficulty with the square well, namely that of obtaining compound nucleus formation cross sections which are as large as the observed inelastic collision cross sections.

ACKNOWLEDGMENTS

The authors gratefully acknowledge the assistance of Dr. R. G. Thomas in initiating and interpreting the optical model calculations, and of the members of Group T-1 who performed the large number of numerical computations on the IBM-701. Our thanks are also due to Dr. E. D. Cashwell, Dr. C. J. Everett, and to Mr. R. L. Bivins of the Los Alamos MANIAC computing group for performing the Monte Carlo calculations involved in correcting the experimental scattering data. We also wish to thank Dr. W. G. Cross of Chalk River and Dr. J. H. Coon of Los Alamos for the use of their data prior to publication.

[25] L. Rosen and L. Stewart, Phys. Rev. **99**, 1052 (1955).